

# 6 CM OBSERVATIONS OF NONTHERMAL RADIO SOURCES NEAR THE GALACTIC PLANE

By D. K. MILNE\*

[Manuscript received January 13, 1969]

## Summary

Brightness distributions and flux densities at 5000 MHz are presented for 17 nonthermal sources (possible supernova remnants) together with their spectra derived from these and other observations. For most sources a comparison has been made between the brightness distribution at 5000 MHz and that obtained with comparable resolution at 408 MHz with the Molonglo 1 mile Cross.

## I. INTRODUCTION

Kesteven (1968*a*) recently published a list of radio sources near the galactic plane observed at 408 MHz with the Mills Cross at the Molonglo Radio Observatory. A further publication (Kesteven 1968*b*) has provided maps of many of those objects that were shown to have nonthermal spectra. This paper describes radio observations made at 5000 MHz with the ANRAO 210 ft telescope at Parkes for 16 of the objects in Kesteven's catalogue and 1 object (MSH 11-54) not catalogued by Kesteven. At 5000 MHz the resolution obtained with the 210 ft telescope is comparable with that of the Mills Cross, so that changes in spectra over an object can be determined from a direct comparison of the brightness distributions.

## II. EQUIPMENT

The 5000 MHz receiver was a cryogenically refrigerated Airborne Instruments Laboratory parametric amplifier with Dicke switching between aerial and cold termination. It was made available by the National Radio Astronomy Observatory, Greenbank, West Virginia. This receiver when installed on the 210 ft telescope provided a total system noise temperature of 120°K over a bandwidth of 250 MHz. With a 1 sec integration time the r.m.s. noise was about 0.05°K in brightness temperature.

The aerial and receiver were calibrated from observations of a point source Hydra A, for which a flux density  $S$  of 13 f.u.† was assumed. The half-power beamwidth  $b$  measured on this point source (and others) was 3.95 min arc; the beam was circular. The brightness-temperature ( $T_b$ ) scale used in this paper was then derived from the expression

$$S = (2k/\lambda^2) \iint_{\Omega} T_b d\Omega, \quad (1)$$

\* Division of Radiophysics, CSIRO, P.O. Box 76, Epping, N.S.W. 2121.

† 1 flux unit =  $10^{-26} \text{ W m}^{-2} \text{ Hz}^{-1}$ .

which for a Gaussian beam can be expressed as

$$S = (2k/\lambda^2) \times 1.13b^2T_b. \quad (2)$$

### III. OBSERVATIONS

The regions containing each source were scanned, usually in declination, at drive rates such that at least six time constants were contained in each beamwidth. The scans were spaced at approximately half-beamwidth intervals. Only one polarization was used in these surveys, at the  $E$  vector position angle quoted in the legend for each map. Polarization data are not available for most of the sources investigated and no attempt has been made to allow for polarization in the brightness isotherms or in the estimated flux densities. It is hoped that the specification of errors will allow for any effect that polarization might produce in these estimates. The results of polarization measurements are given in Figure 10 and Table 4 for two sources, CTB37 and W44 (see Milne (1968*b*) for details of the observational and data reduction techniques used).

For all but three of the sources (MSH 11—54, 3C391, and 4C—03-70) isotherms have been constructed and integrated to determine the flux density. These three sources were found to have simple Gaussian brightness distributions, and their integrated flux densities  $S_{\text{int}}$  followed from the relationship

$$S_{\text{int}} = S_{\text{peak}}(W/b)^2, \quad (3)$$

where  $W$  is the half-intensity width of the Gaussian fitted to the observed profile and  $b$  the antenna beamwidth.

The errors quoted in estimates of the flux density are fairly subjective, the largest source of error being the determination of the baselevel over which the integration should be carried out. The flux estimate for the simplest source should be within  $\pm 5\%$ , and for the most complex within  $\pm 20\%$ .

The brightness distributions given here are isotherms of brightness temperature multiplied by a constant which varies from map to map (quoted in the legend for each).

For two of the sources studied (Kepler's Nova and 3C391) supporting observations were made using the Parkes interferometer at 470 and 1410 MHz (see Ekers (1969) for a description of this instrument and the observing techniques used). The visibility functions are presented in Figures 11 and 15 and interpretations of these are given in the following discussion of the 5000 MHz results for each of the sources observed.

### IV. DISCUSSION OF RESULTS

Table 1 gives the 5000 MHz positions, angular sizes, and flux densities for the sources observed in this investigation, while Table 2 gives the flux densities measured by other observers, and includes Kesteven's catalogue numbers and the present 5000 MHz flux densities from Table 1. The spectral indices suggested by these data are also given in Table 2; the spectra are displayed graphically in Figures 1( $a$ )–1( $e$ ).

TABLE 1  
5000 MHz RESULTS FOR NONTHERMAL SOURCES NEAR GALACTIC PLANE

Galactic Catalogue Number	Common Name	Components	Gal. Coords $l_{II}$ °	$b_{II}$ °	Position (1950) R.A. h m s	Dec. °	Angular Size	Flux Density (f.u.)
290-1-0-8	MSH 11-61	A	290-11	-0-76	11 00 45	-60 38-0	13' R.A. × 12' Dec.	28 ± 15%
		B	289-89	-0-79	10 59 02	-60 33-8	4' × 1' 5".2	6 ± 10%
		A+B	290-1	-0-8	11 00 29	-60 37-0	23' × 12', P.A. 115°	34 ± 15%
292-0+1-8	MSH 11-54		292-03	+1-76	11 22 21	-58 59-4	2' × 8 R.A. × 2' × 7 Dec.	8-3 ± 5%
295-2-0-6			295-15	-0-61	11 40 57	-62 10-4	9' × 4".2, P.A. 45°; extensive wings to 16' diam.	10-7 ± 15%
304-6+0-1			304-58	+0-11	13 02 39	-62 26-7	5'.2 R.A. × 6'.1 Dec.	6-8 ± 10%
309-7+1-7	MSH 13S6A	A	309-75	+1-75	13 43 33	-60 08-3	7'.1 × 5'.4, P.A. 45°	33 ± 10%
		B	309-62	+1-68	13 42 42	-60 13-9	6'.3 diam.	17 ± 10%
		A+B	309-7	+1-7	13 43 19	-60 11-8	14' × 5', P.A. 45°	50 ± 10%
310-8-0-4		A	310-83	-0-44	13 56 32	-62 00-8	8' × 11'	9
		B	310-64	-0-32	13 54 41	-61 56-6	7'.5 diam.	3
		A+B	310-76	-0-37	13 55 45	-60 57-5	24' × 13'	12 ± 30%
326-2-1-7	MSH 15-56		326-21	-1-73	15 48 26	-56 02-8	10'.9 × 8'.6, P.A. 135°; full diam. ~ 30'	98 ± 10%
332-4+0-1	MSH 16-51	Peak	332-45	+0-11	16 11 48	-50 33-2	18' × 10', P.A. 120°; full diam. ~ 22'	12-3 ± 15%
332-4-0-4	RCW 103	Centroid	332-40	-0-40	16 13 47	-50 57-4	7'-0 R.A. × 7'-9 Dec.	12-6 ± 15%
		A	332-41	-0-38	16 13 44	-50 56-0		
		B	348-48	+0-09	17 11 12	-38 26-7		
348-5+0-2	CTB 37	A+B	348-68	+0-35	17 10 47	-38 07-7	8'.1 × 5'.8	39-1 ± 10%
			348-5	+0-2	17 11 06	-38 20-9	3'.8 × 6'-0	22-0 ± 10%
4-5+6-8	Kepler's Nova		4-53	+6-82	17 27 43	-21 26-8	2'.19 diam.	61-1 ± 10%
							1'.5 shell (interferometer)	7-1 ± 8%
18-8+0-3	MSH 18-18	Peak	18-86	+0-33	18 21 21	-12 22-2		
		Centroid	18-81	+0-32	18 21 17	-12 25-1	7' R.A. × 14' Dec.	15-1 ± 15%
23-1-0-0	W 41	Peak	23-43	-0-21	18 32 00	-08 35-0	Possible shell 1° × 11° diam. emission concentrated to 45' × 60' region	225 ± 20%
		Centre of shell	23-08	-0-01	18 30 38	-08 48-0		
27-3-0-0		A	27-40	-0-01	18 38 41	-04 58-8	2'.2 × 2'.6	1-44
		B	27-28	-0-15	18 37 54	-05 00-2	1'.8 × 1'.1	1-63
		C	27-51	-0-14	18 38 23	-04 47-5	4'.5 diam.	
		D	27-30	-0-20	18 39 10	-05 08-5		
29-7-0-2	4C-03-70	A+B+C+D	27-34	-0-02	18 38 30	-05 01	32' diam.	23 ± 20%
31-9+0-0	3C 391		29-70	-0-25	18 43 49	-03 02-1	2'.2 R.A. × 1'.2 Dec.	3-3 ± 8%
			31-87	+0-04	18 46 47	-00 58-7	3'.7 × 3'.1	10 ± 8%
34-6-0-5	W 44	Peak	34-65	-0-59	18 54 08	+01 11-4	3'.6 × 3'.5 (interferometer)	149 ± 15%
		Centroid	34-63	-0-49	18 53 45	+01 13-0	28' × 35'	
							20' diam. shell	

FLUX DENSITIES OF NONTHERMAL SOURCES NEAR GALACTIC PLANE

Galactic Catalogue Number	Kes. No.*	408*	5000†	86	159	178	408	635	960	1390	1410	1440	2650 MHz	Spectral Index
Flux Density (f.u.)†														
290-1-0-8A	13	170	28 ± 15%											
B			6 ± 10%	178(1)			160(2)			80(3)		100(4)		-0.63
A+B			34 ± 15%	[162]§			[148]§							
292-0+1-8	Not catalogued		8.3 ± 5%	39(1)			19(2)	17 ± 10%(17)					10.3 ± 10%(17)	-0.36
295-2-0-6	16	40	10.7 ± 15%											-0.60
304-6+0-1	17	21	6.8 ± 10%											-0.50
309-7+1-7A			33 ± 10%											
B			17 ± 10%											
A+B	19	210	50 ± 10%	795(1)			242(2)						60 ± 10%(5)	-0.65
310-8-0-4A	20	22	9											-0.35(?)
B	{15}	37	12 ± 30%											-0.65
A+B	25	170	98 ± 10%	323(1)									40 ± 30%(3)	-0.6
326-2-1-7				[270]§									130(4)	-0.24
332-4+0-1	32	23	12.3 ± 15%	256(1)									14(7)	-0.45(?)
332-4-0-4	33	30	12.6 ± 15%										15(7)	-0.34
348-5+0-2A	47	124	39.1 ± 10%										51 ± 10%(5)	-0.44
B	48	72§	22.0 ± 10%										28 ± 10%(5)	-0.49
(orig. 36)														
A+B	57	196	61.1 ± 10%										79 ± 10%(5)	-0.51
4-5+6-8	67	{70}	7.1 ± 8%	150(1)										-0.58
18-8+0-3			15.1 ± 15%											-0.57
23-1-0-0	70	Part only	225 ± 20%	440(1)			560(15)		225(15)	334(14)			365 ± 25%(12)	-0.22
27-3-0-0A	73	11	1.44	[160]§			[265]		[75]§	[75]§				-0.7
B			1.63											
C														
A+B+C+D	75	11	7.7(16)	20(1)	22(10)								3(9)	-0.27
29-7-0-2	77	27	23 ± 20%										3(9)	-0.14
31-9+0-0			3.3 ± 8%										28 ± 15%(9)	-0.5
			10 ± 8%	20(1)	27 ± 22%(10)								11(9)	-0.5
													13.3(9)	-0.5
													[11]§	-0.40

\* Kesteven (1968a, 1968b); values in braces were estimated from his (1968b) contours.

† Present results from Table 1.

‡ References are: (1) Mills, Slee, and Hill (1958, 1960, 1961); (2) Komesaroff (1966); (3) estimated from Hill's (1963) isotherms; (4) Mathewson, Healey, and Rome (1962); (5) Milne and Hill (1969); (6) Hill (1967); (7) Beard, Scott, and Willis (1967); (8) Gower, Scott, and Willis (1969); (9) Beard and Kerr (1969); (10) Edge *et al.* (1968); (11) Bennett (1962); (12) Day (personal communication, see text); (13) Davis, Gelato-Volders, and Westerhout (1965); (14) Westerhout (1958); (15) Wilson (1963); (16) Reitenstein (1968); (17) previous unpublished measurements by author, see Milne and Hill (1969); (18) Beard (personal communication).

§ Flux densities originally quoted were either peak values (shown in square brackets) or integrated values based on incorrect angular sizes; they have been adjusted for extent using the angular sizes given in the present paper.

Optical plates and prints have been searched for possible associated nebulae. For the first nine sources in Table 1 several 103aE plates exposed for 90 min with the Uppsala 26 in. Schmidt camera were examined and nebulae were found in the positions of two of the radio sources: MSH 11-61/B and RCW 103 (the latter object has been previously identified). For the other eight sources an examination of the Mount Palomar Sky Survey Atlas showed nebulae in the position of only one object: Kepler's Nova. These nebulae are marked on the contour maps. A discussion of the results, source by source, follows.

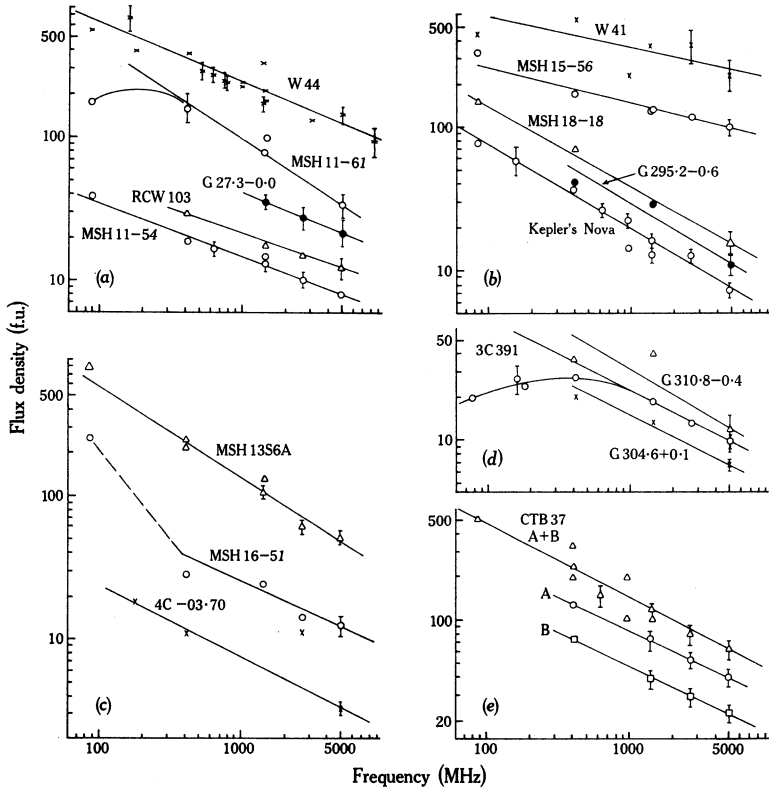


Fig. 1.—Spectra of the 17 sources investigated based on the data given in Table 2.

(a)  $G290.1-0.8$ , MSH 11-61, Kes 13

The 5000 MHz isotherms in Figure 2 show MSH 11-61 to consist of two components separated by 14 min arc with 82% of the flux in the major component. It is to be noted that Kesteven (1968*b*) does not include the minor component B in his map of 11-61 and presumably not in his integrated flux density (Kesteven 1968*a*). The position measured by Mills, Slee, and Hill (1961) for 11-61 suggests that component B (the minor component at 5000 MHz) might have a steeper spectrum

than A. The spectrum of component A between 408 and 5000 MHz is certainly non-thermal and that of both together nonthermal with a spectral index of  $\alpha = -0.63$ . This latter spectrum, constructed from the data of Table 2, is shown in Figure 1(a). There are indications of absorption at 86 MHz. The 26 in. Schmidt plate for this region shows patches of nebulosity in the position of component B. These nebulae are sketched in Figure 2.

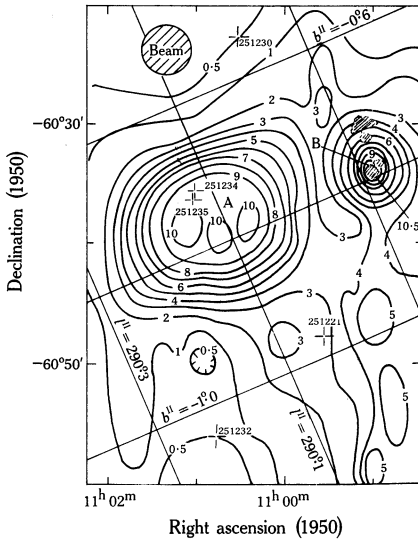


Fig. 2.—5000 MHz isotherms for G290.1-0.8 (MSH 11-6I). The contour unit is 0.233°K in  $T_b$  and the  $E$  vector position angle is 75°. The shaded areas indicate the positions of nebulae near MSH 11-6I/B, while the positions of bright stars in this field are also shown together with their Smithsonian catalogue numbers.

(b)  $G292.0+1.8$ , MSH 11-54

This source is fairly isolated from the galactic ridge. It is clearly nonthermal with  $\alpha = -0.36$ . This fairly flat spectrum, together with the circular shape and moderate size (nearly 3 min arc), suggests that the object is galactic rather than extragalactic.

(c)  $G295.2-0.6$ , Kes 16

The 5000 MHz isotherms (Fig. 3) agree well with those at 408 MHz (Kesteven 1968b). There is at both frequencies an elongation in the central part of the source along a position angle of 45°; the wings in both maps extend to about 16 min arc diameter.

(d)  $G304.6+0.1$ , Kes 17

The faint suggestion of a shell present in Kesteven's isotherms is not evident in the 5000 MHz contours of Figure 4.

(e)  $G309.7+1.7$ , MSH 1386A, Kes 19

The 5000 MHz contours of this source (Fig. 5) are similar to those given by Kesteven at 408 MHz. A comparison of the peak temperatures between the two maps yields similar nonthermal spectra for each component ( $\alpha = -0.78$  for

component A and  $-0.81$  for component B). However, there is a displacement of the peak of component A along the major axis towards the south-west with increasing frequency. This displacement (3 min arc between 408 and 5000 MHz) means that the spectral index is much steeper at the north-east extreme than elsewhere in the source.

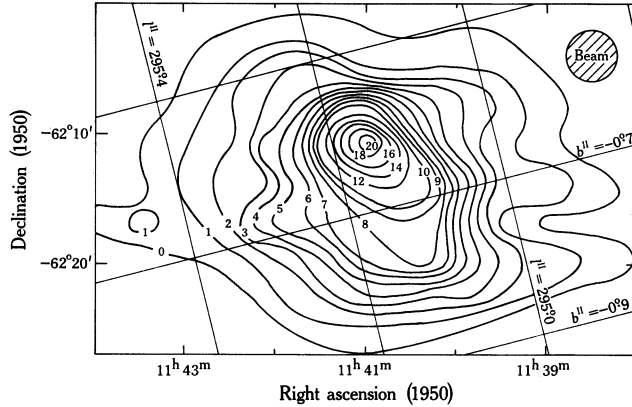


Fig. 3.—5000 MHz isotherms for G295.2-0.6. The contour unit is  $0.245^{\circ}\text{K}$  in  $T_b$  and the  $E$  vector position angle is  $90^{\circ}$ .

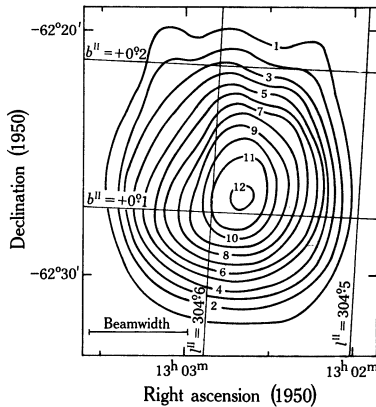


Fig. 4.—5000 MHz isotherms for G304.6+0.1. The contour unit is  $0.183^{\circ}\text{K}$  in  $T_b$  and the  $E$  vector position angle is  $25^{\circ}$ .

The source 13S6A has not been optically identified. It is, however, similar in structure and spectrum to certain extragalactic sources and no evidence has yet been given for placement of this source within the Galaxy.

(f) *G310.8-0.4, Kes 20*

The 5000 MHz contours for this source (Fig. 6) show two components A and B. In this respect there is a similarity between the object mapped by Kesteven (1968*b*) at 408 MHz and Figure 6, although the shell structure in component A at 408 MHz

is not apparent at 5000 MHz. From the size and position given in Kesteven (1968*a*) and the present estimates of the flux for this source we assume that Kes 20 is only the major component of this pair. The present estimate (from Kesteven 1968*b*) of the 408 MHz flux density of the minor component B is 15 f.u., which with the flux

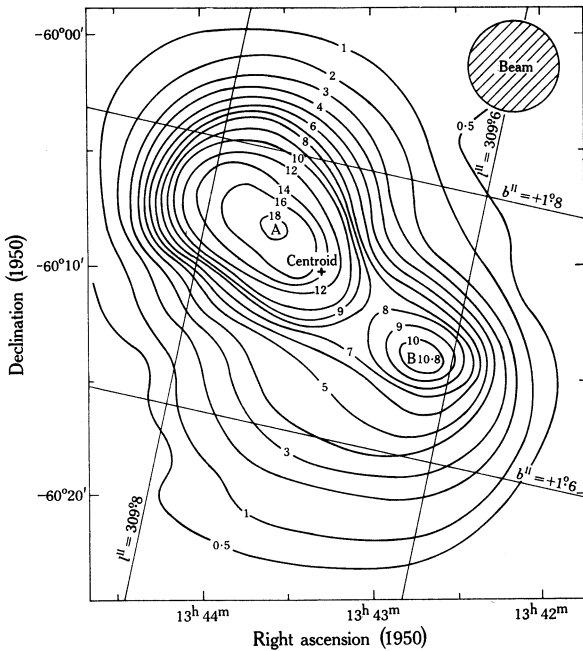


Fig. 5.—5000 MHz isotherms for G309.7+1.7 (MSH 13S6A). The contour unit is 0.46°K in  $T_b$  and the  $E$  vector position angle is 30°. The 5000 MHz centroid is indicated.

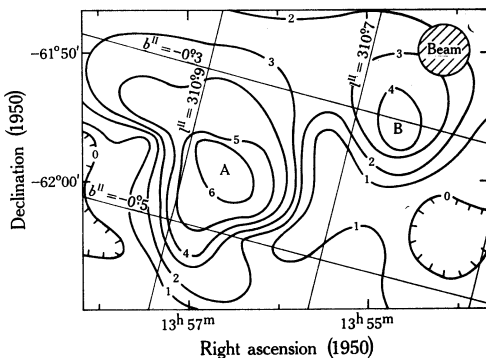


Fig. 6.—5000 MHz isotherms for G310.8-0.4. The contour unit is 0.21°K in  $T_b$  and the  $E$  vector position angle is 80°. The source Kes 20 is the major component (A) of this pair.

density of 3 f.u. measured at 5000 MHz would give B a nonthermal spectrum. Component A is also nonthermal but not as steep as component B, although the former spectrum is influenced by Kesteven's 408 MHz flux density for A, which is possibly an underestimate. This is also suggested by the present estimate of the 1410 MHz flux (from Hill 1968) for components A and B. This latter result, together with the

5000 MHz result, would give components A and B together a very steep spectrum ( $\alpha = -0.9$ ), whilst between 408 and 5000 MHz the spectral index is  $-0.45$ . We conclude that both components probably have similar spectral indices of about  $-0.6$ .

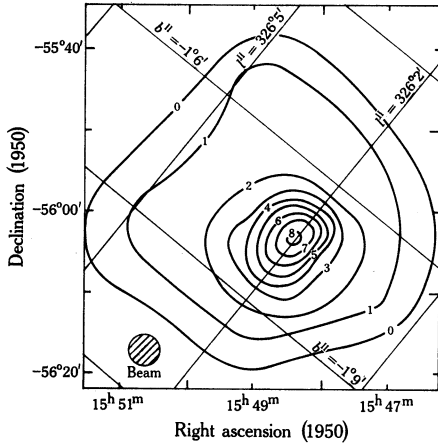


Fig. 7 (left).—5000 MHz isotherms for G326.2-1.7 (MSH 15-56). The contour unit is  $0.75^\circ\text{K}$  in  $T_b$  and the  $E$  vector position angle is  $65^\circ$ . The isotherms show a central concentration surrounded by extensive wings.

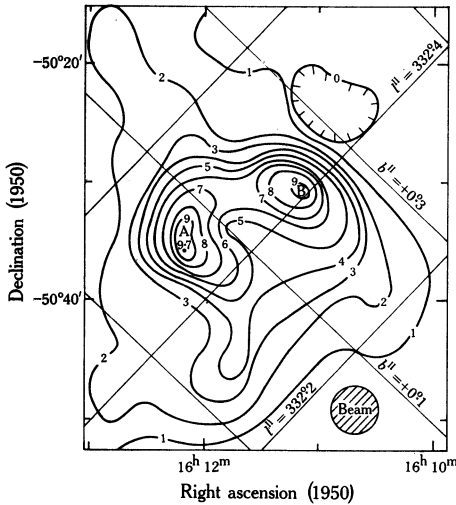


Fig. 8.—5000 MHz isotherms for G332.4+0.1 (MSH 16-5I). The contour unit is  $0.215^\circ\text{K}$  in  $T_b$  and the  $E$  vector position angle is  $85^\circ$ . The shape of the isotherms suggests a shell with two prominent peaks, A and B.

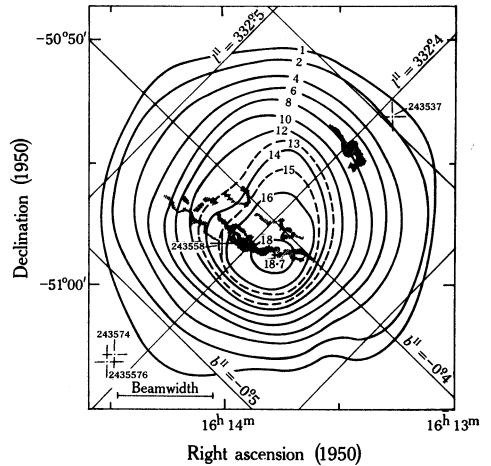


Fig. 9.—5000 MHz isotherms for G332.4-0.4 (RCW 103). The contour unit is  $0.19^\circ\text{K}$  in  $T_b$  and the  $E$  vector position angle is  $75^\circ$ . The shaded areas indicate the filaments noted by Westerlund (Beard 1966) and the crosses give the positions of bright stars in the Smithsonian catalogue.

(g) G326.2-1.7, MSH 15-56, Kes 25

There is a similarity between the 5000 MHz contours (Fig. 7) and Kesteven's 408 MHz map in that there is an extension of the outer contours towards the north-east and an elongation of the inner contours along a position angle of  $135^\circ$ . This

source consists of a central core (diameter  $10' \cdot 9 \times 8' \cdot 6$ ) with extensive wings out to a full diameter of about  $30'$ . The spectrum of this source is fairly flat (Fig. 1(b)) but it is undoubtedly nonthermal.

(h)  $G332 \cdot 4 + 0 \cdot 1$ , MSH 16—51, Kes 32

The shape of the isotherms at both 408 and 5000 MHz (Fig. 8) suggests that this source may consist of a shell with two prominent peaks of emission. The spectrum is slightly flatter on the most western of the two peaks.

(i)  $G332 \cdot 4 - 0 \cdot 4$ , RCW 103, Kes 33

A fairly similar structure emerges at both 408 and 5000 MHz (Fig. 9) but Kesteven defines a possible shell more clearly than is shown at 5000 MHz. This source has been identified optically (Beard 1966; Kesteven 1968*b*) with two filaments running parallel at a position angle of  $45^\circ$ . The position of these is indicated in Figure 9.

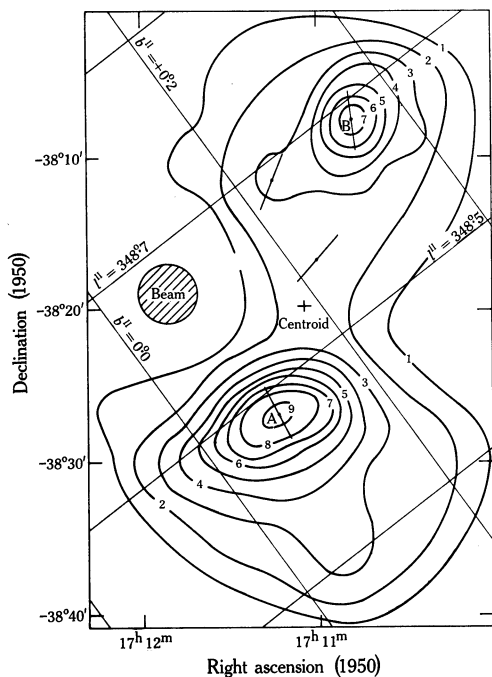


Fig. 10.—5000 MHz isotherms for  $G348 \cdot 5 + 0 \cdot 2$  (CTB 37). The contour unit is  $0 \cdot 75^\circ\text{K}$  in  $T_b$  and the  $E$  vector position angle is  $115^\circ$ . The 5000 MHz centroid position and the direction of the  $E$  vector at four positions in the source are indicated:

Position (1950)			Position	Polari-
R.A.	Dec.	Angle	zation	
h m s	° ' "	(degrees)	(%)	
17 10 48	-38 07.3	28	1.6	
17 11 14	-38 11.6	159	1.1	
17 11 01	-38 17.7	137	8.0	
17 11 12	-38 26.5	2	2.1	

(j)  $G348 \cdot 5 + 0 \cdot 2$ , CTB 37, Kes 47 and 48

At 5000 MHz (Fig. 10) the components of this double source are well resolved and some structure is visible in each component. There is an elongation of component B along the major axis of the pair, which are linked by emission along this axis. Polarization measurements were made at four points within this source yielding the position angles and percentages of linear polarization given in the legend to Figure 10. The similar polarization in each component and the high percentage polarization on

the bridge between the sources support the suggestion that the two sources are physically related.

The spectrum of each component and that of the two together have been plotted in Figure 1(e); the spectral index for each is similar. Note that the flux density of Kesteven (1968*a*) has been increased for component B to allow for the larger diameter estimated at 5000 MHz. The validity of this correction follows from a comparison of the total flux at 408 MHz estimated by other observers (see Milne and Hill 1969) and that given by Kesteven.

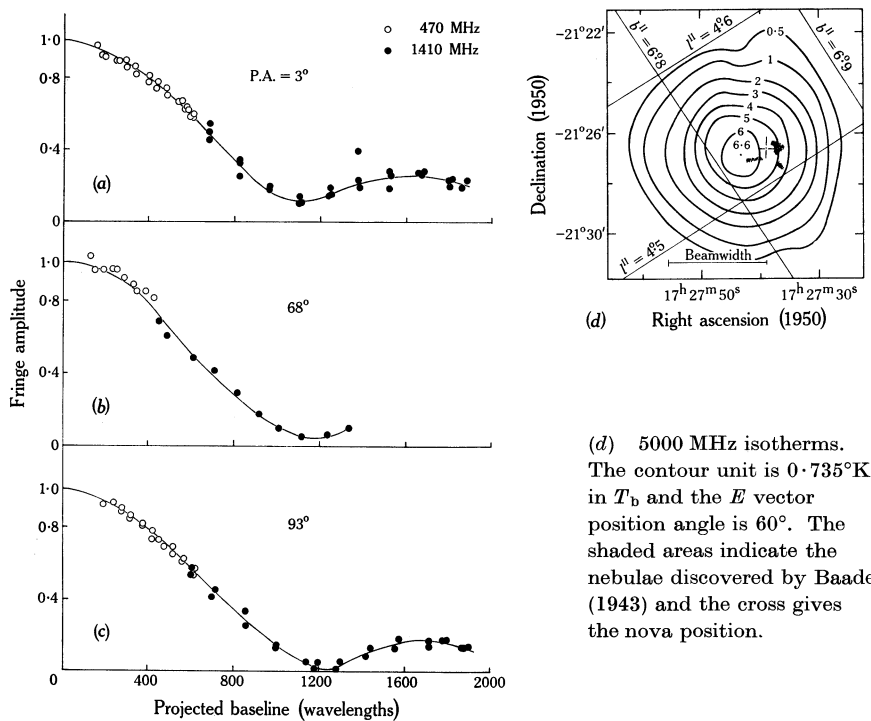


Fig. 11.—Showing for G4.5+6.8 (Kepler's Nova): (a)–(c) Fringe amplitudes at two frequencies and at three fringe position angles. The data for (a) were derived from three baseline runs with the north–south interferometer and for (b) and (c) from one run and two runs respectively with the east–west interferometer. It is thought, from the relative phase between the 470 and 1410 MHz fringes, that the central and second maximum are of opposite phase (see text for interpretation).

Whether this object is within the Galaxy has not been established. The existence of a physical relationship between the two sources appears to be certain, and it has been suggested (Milne 1968*a*) that CTB 37 is a galaxy similar to Fornax A. Certainly there is a striking similarity between the structure of both of these objects (see, for example, Morimoto and Lockhart 1968).

*(k) G4·5+6·8, Kepler's Nova, Kes 57*

The 5000 MHz observations presented here for this source (and 3C 391) have been supported by measurements made with the Parkes interferometer. Figures 11(a)–11(c) present the fringe visibility functions obtained for Kepler's Nova for three different position angles. The tentative interpretation of these is in terms of an emission ring, presumably the projection of a shell, of mean diameter  $1'·5$  and thickness  $1'·1$ . When convolved with the  $3'·95$ , 5000 MHz beam this model would appear as a Gaussian source of  $4'·5$  half-power width, identical with that measured at 5000 MHz in this investigation. The 5000 MHz isotherms (Fig. 11(d)) show some departures from symmetry which are outside the expected errors, indicating that there is further structure beyond the suggested emission ring. The flux density obtained from an integration of this map is given in Table. 2. The spectrum obtained from these data, together with those given by Milne and Hill (1969), is plotted in Figure 1(b); a power-law spectrum of  $\alpha = -0·58$  is indicated. In Figure 11(d) the nebulosities found by Baade (1943) in the position of Kepler's Nova are indicated. The region enclosed by these nebulae is comparable in size to that of the radio source but their centroid position differs from that of the radio source by  $0'·7$ .

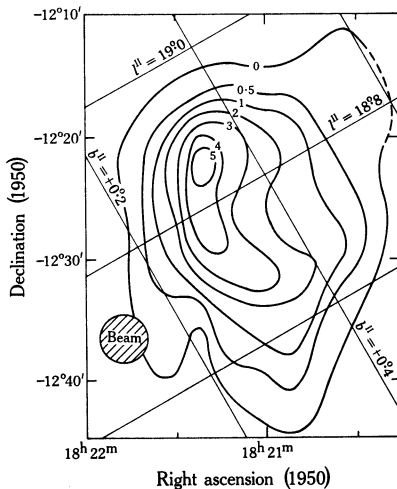


Fig. 12.—5000 MHz isotherms for G18·8+0·3 (MSH 18–18). The contour unit is  $0·36^{\circ}\text{K}$  in  $T_b$  and the  $E$  vector position angle is  $120^{\circ}$ .

*(l) G18·8+0·3, MSH 18–18, Kes 67*

There is a marked similarity between the 408 and 5000 MHz maps (Kesteven 1968b) and Figure 12. There are two errors in Kesteven (1968a) in respect to this source: it is the same as MSH 18–18, not 18–19, and the 408 MHz angular size as shown by Kesteven's map is approximately  $15' \times 7'$ , not  $6'·6$  diameter. A comparison of the 408 MHz flux density measured by Kesteven with that expected from Mills, Slee, and Hill (1958) and the 5000 MHz flux suggests that Kesteven's estimate is low by a factor of two. This may have been due to his underestimated angular size. In the present work the integrated 408 MHz flux density has been estimated from Kesteven's isotherms and this is the value given in Table 2 and Figure 1(b). The

brightness distribution over this source suggests a partial shell of mean diameter  $13'$  arc and a deconvolved thickness of about  $2'$  arc.

(m)  $G23\cdot1-0\cdot0$ ,  $W\ 41$ ,  $Kes\ 70$

Kesteven's map of  $W\ 41$  suggests a shell source of mean diameter  $23'$  arc. This shell is indicated in the 5000 MHz map (Fig. 13), but it is not an obvious feature in the contours. There is, however, a possible shell of much larger dimensions ( $\sim 1^\circ$  diameter) centred on R.A.  $18^h 30^m 20^s$ , Dec.  $-08^\circ 47'$  (1950). G. A. Day has kindly made available, in advance of publication, a 2650 MHz,  $8'\cdot4$  beamwidth survey of the

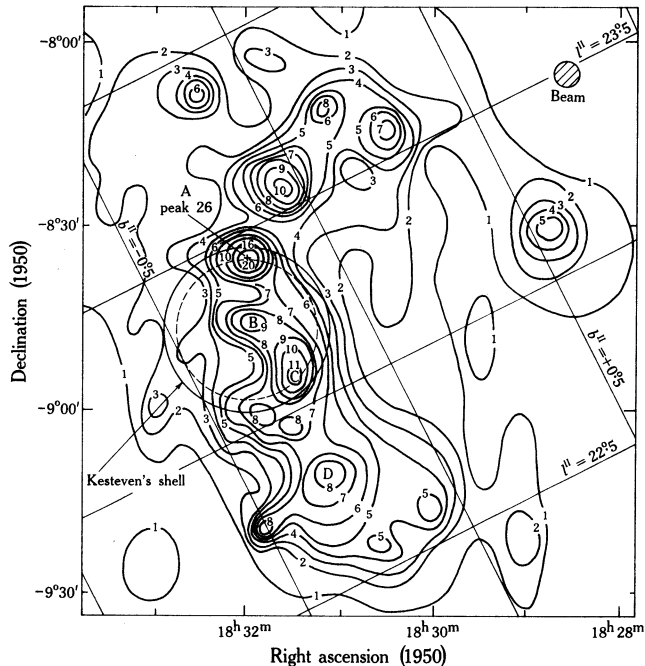


Fig. 13.—5000 MHz isotherms for  $G23\cdot1-0\cdot0$  ( $W\ 41$ ). The contour unit is  $0\cdot246^\circ\text{K}$  in  $T_b$  and the  $E$  vector position angle is  $125^\circ$ . The shell outlined at 408 MHz (Kesteven 1968*b*) is also indicated.

this region from which the author has constructed isotherms of  $W\ 41$ . The integrated flux obtained from this has been included in Table 2. A nonthermal spectrum is indicated between this and the flux at 5000 MHz. Further to this, values of the flux density given by other observers, who with only low resolutions available have underestimated the angular extent of  $W\ 41$ , have been taken and adjusted to an angular extent of  $45'$  in right ascension by  $60'$  in declination, this being the size of the region from which nearly all the emission originates. The spectrum drawn from these modified data is shown in Figure 1(*b*). A fairly flat spectral index ( $-0\cdot22$ ) is indicated, so that the nonthermal nature is still uncertain. Reifenstein (1968) obtained a  $H\ 109\alpha$  recombination line on each of the two sources A and D (see Fig. 13), whilst a third

source C yielded none. This shows that at least part of the object has thermal emission. A comparison of the 5000 and 408 MHz (Kesteven 1968*b*) maps yields spectral indices for the three sources A, B, and C of  $-0.33$ ,  $-0.73$ , and  $-0.60$  respectively, all nonthermal but with B and C steeper than the one exhibiting the H 109 $\alpha$  line (source D is outside the region mapped by Kesteven); the errors are large in a comparison such as this.

An extension of the 408 MHz observations together with the present 5000 MHz observations would determine the nature of W 41. The present suggestion is, however, that it is a supernova remnant with a well-defined shell of about  $50' \times 70'$  mean diameter and thickness  $18'$ .

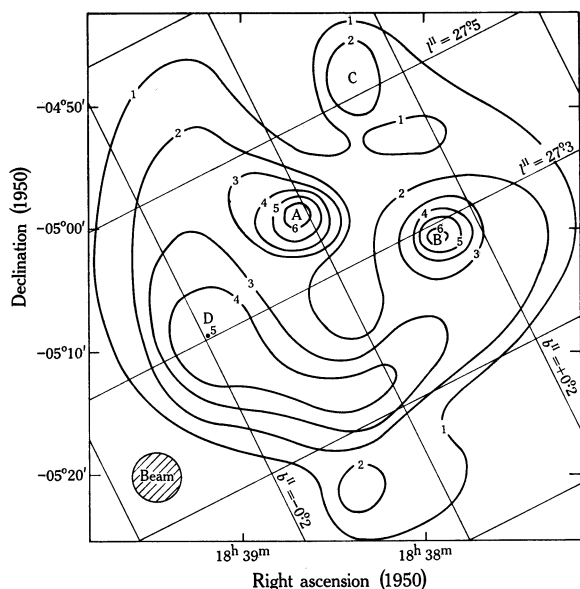


Fig. 14.—5000 MHz isotherms for G27.3—0.0 (3C 387). The contour unit is  $0.21^\circ\text{K}$  in  $T_b$  and the  $E$  vector position angle is  $145^\circ$ . The source Kes 73 is labelled A here.

(n) G27.3—0.0, 3C 387, Kes 73

The 5000 MHz map of the region about Kes 73 (Fig. 14) shows this source as part of a larger complex which has some of the structural characteristics of the well-established supernova remnants. This complex consists of two prominent small diameter sources, A (Kes 73) and B, superimposed on a loop of emission that has its peak in source D, while there is a weak  $4.5'$  diameter source C to the north.

The whole complex appears as an isolated object in the 2650 and 1410 MHz maps of Beard and Kerr (1969) of this part of the galactic plane. The integrated flux densities of the whole source obtained from these maps are  $28 \text{ f.u.} \pm 20\%$  and  $35.8 \text{ f.u.} \pm 15\%$  respectively (Beard, personal communication) and these, together with the integrated flux density at 5000 MHz, yield a spectral index of  $-0.4$  (see Fig. 1(a)), so that G27.3—0.0 is clearly a nonthermal source.

Various estimates of the flux density of the component sources are given in Table 2. It has been possible to derive a spectral index from these for two of the sources, A ( $\alpha = -0.7$ ) and D ( $\alpha = -0.27$ ). It is to be noted that the flatter of these

(D) shows the presence of a  $H\ 109\alpha$  recombination line and is presumably thermal (Reifenstein 1968). The present indications are that this complex is a supernova remnant. It would be advantageous to extend the 408 MHz observations to cover the entire object.

(o)  $G29.7-0.2$ ,  $4C-03.70$ ,  $Kes\ 75$

This object appeared in the 5000 MHz scans as a single Gaussian source with deconvolved diameters  $2'.2$  in right ascension and  $1'.2$  in declination and no map was constructed. The flux density estimated at 2650 MHz (Beard and Kerr 1969) is too high; otherwise the flux densities given in Table 2 readily define a power-law spectrum with  $\alpha = -0.53$ . This source is possibly extragalactic.

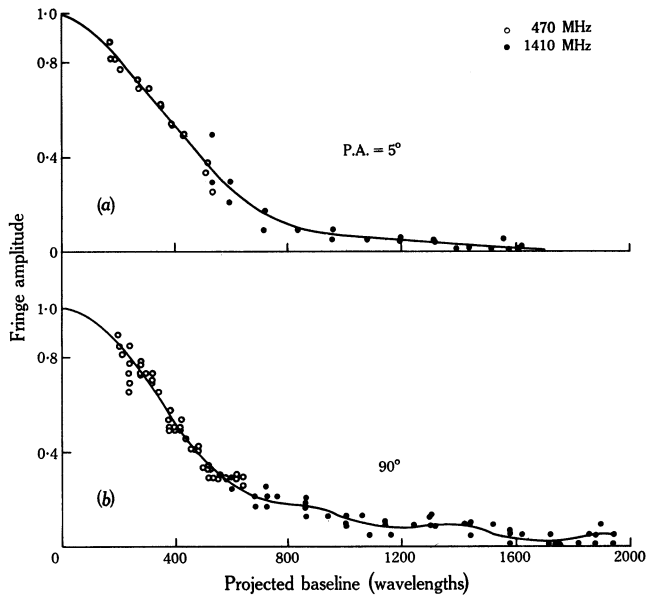


Fig. 15.—Fringe amplitudes for  $G31.9-0.0$  (3C 391) at two frequencies and at two fringe position angles. The data for (a) were derived from two runs along the north-south baseline and for (b) from four runs with the east-west interferometer. The interpretation of these is discussed in the text.

(p)  $G31.9+0.0$ ,  $3C\ 391$ ,  $Kes\ 77$

The source 3C 391 appears at 5000 MHz as a fairly symmetrical Gaussian source of deconvolved angular size  $3'.7$  in right ascension by  $3'.2$  in declination. The right ascension scan shows small departures from a Gaussian profile with a slight extension of the source towards the east. The interferometric visibility functions obtained for this source (Fig. 15) can be interpreted with a Gaussian source model of half-power width  $3'.6$  (R.A.) by  $3'.5$  (Dec.). There is a weak confusing source ( $S \sim 0.5$  f.u.) near a position angle of  $90^\circ$  and having a projected separation from the main source of  $7'.3$  in this direction.

The spectrum of 3C 391 (Fig. 17(d)) is of interest. It is nonthermal with a considerable amount of absorption below 900 MHz. At this frequency the temperature of the absorber must equal the brightness temperature of the source. From equation (2), for  $\lambda = 0.33$  m,  $S = 23$  f.u. and  $b = 10^{-3}$  rad, we arrive at a temperature of  $830^\circ\text{K}$  for the absorbing medium. At 86 MHz the optical depth, given by the ratio of the measured flux to that expected from an extrapolation of the high frequency measurements, is 1.42, which, if free-free (thermal) absorption is adopted, requires that the emission measure of the absorbing material between the Sun and the source be  $620 \text{ cm}^{-6} \text{ pc}$ , for an electron temperature of  $830^\circ\text{K}$ .

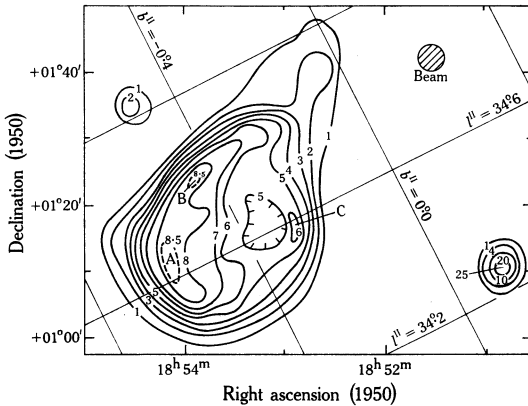


Fig. 16.—5000 MHz isotherms for G34.6—0.5 (W 44). The contour unit is  $0.49^\circ\text{K}$  in  $T_b$  and the  $E$  vector position angle is  $150^\circ$ . The 5000 MHz polarization results for this source are given in Table 4.

(q) G34.6—0.5, W 44, Kes 80

The 5000 MHz isotherms (Fig. 16) are quite similar to the map of Kesteven (1968b) at 408 MHz. The 5000 MHz contours show an extension to the north and to the south, suggesting that the source is thermal in these extremities. The spectrum between 408 and 5000 MHz is nonthermal around the ridge ( $\alpha = -0.5$  at the peaks A, B, and C; see Fig. 16) whilst it is thermal ( $\alpha = +0.1$ ) in the central depression. This is consistent with the spectrum obtained from the integrated flux densities of Table 3 for which  $\alpha = -0.4$  (Fig. 1(a)). The source to the west of W 44 at R.A.  $18^{\text{h}} 50^{\text{m}} 49^{\text{s}}$ , Dec.  $+01^\circ 10' 3$  (1950) has a 5000 MHz flux density of  $13.2 \text{ f.u.} \pm 8\%$ , and in agreement with Hollinger and Hobbs (1966) it is judged that this source is thermal. The other isolated source (R.A.  $18^{\text{h}} 54^{\text{m}} 34^{\text{s}}$ , Dec.  $+01^\circ 34' 5$  (1950)) was estimated to have a flux density of  $5.8 \text{ f.u.} \pm 8\%$  at 5000 MHz. Its spectrum is unknown but probably it also is thermal.

The position angles and percentage polarizations obtained at two positions in W 44 are given in Table 4, together with those obtained at 8350 MHz by Hollinger and Hobbs (1966) with a  $10'.8$  beam. Allowing for beam smoothing, the results given in Table 4 could be consistent. If we take the average polarization at 5000 MHz to be at approximately  $80^\circ$  position angle and compare this with the 8350 MHz result, we obtain an intrinsic position angle of  $20^\circ$  for the electric vector and a probable

rotation measure of  $+260 \text{ rad m}^{-2}$ . The depolarization would be very high. This is consistent with the high rotation measure and the absence of polarization at 2650 MHz and lower frequencies (Davies and Gardner 1966). Further observations are needed before any real conclusions can be drawn about the polarization and magnetic structure.

TABLE 3  
W 44 FLUX DENSITIES

Frequency (MHz)	Flux Density (f.u.)	Reference
86	550	Mills, Slee, and Hill (1958)
159	$680 \pm 18\%$	Edge <i>et al.</i> (1958)
178	400	Bennett (1963)
408	390	Kesteven (1968 <i>a</i> )
513	$297 \pm 10\%$	Kuzmin (1962)
610	$275 \pm 10\%$	Moran (1965)
740	$249 \pm 6\%$	Kuzmin (1962)
750	$242 \pm 10\%$	Pauliny-Toth, Wade, and Heeschen (1966)
960	$230 \pm 6.5\%$	Kuzmin (1962)
960	240	Wilson (1963)
1390	330	Westerhout (1958)
1400	$171 \pm 12\%$	Pauliny-Toth, Wade, and Heeschen (1966)
1410	215	Scheuer (1963)
1420	180	Leslie (1960)
3000	135	Scheuer (1963)
5000	$149 \pm 15\%$	Present paper
8350	$95 \pm 24\%$	Hollinger and Hobbs (1966)

TABLE 4  
POLARIZATION DATA FOR W 44

Position (1950)				Frequency (MHz)	Beamwidth (min of arc)	Position Angle (degrees)	Polarization (%)
R.A.		Dec.					
h	m	s	°				
18	53	50	+01 18.5	5000	3.95	100	6
18	54	04	+01 08.5	5000	3.95	40	1.5
18	53	54	+01 12.1	8350	10.8	45	11

## V. CONCLUSIONS

For most of the sources studied there is a fairly strong similarity between the 5000 MHz brightness distribution and that obtained by Kesteven (1968*b*) at 408 MHz. Some of the differences can be attributed to the more difficult observing techniques with the Molonglo Cross for large diameter sources. The general tendency for the sources to assume a shell structure in Kesteven's maps is not found in most of the 5000 MHz measurements.

It is believed that of the 17 sources observed 3 are possibly extragalactic (13S6A, CTB37, and 4C-03.70) and the remainder are supernova remnants.

## VI. ACKNOWLEDGMENTS

The NRAO cryogenic parametric amplifier was made available at Parkes by courtesy of Dr. D. S. Heesch. The author is grateful to Dr. G. Lyngå of the Uppsala Southern Station, Mount Stromlo, for providing photographic plates of many of the regions in this investigation.

## VII. REFERENCES

- BAADE, W. (1943).—*Astrophys. J.* **97**, 119.  
 BEARD, M. (1966).—*Aust. J. Phys.* **19**, 141.  
 BEARD, M., and KERR, F. J. (1969).—*Aust. J. Phys.* **22**, 121.  
 BENNETT, A. S. (1962).—*Mem. R. astr. Soc.* **68**, 163.  
 BENNETT, A. S. (1963).—*Mon. Not. R. astr. Soc.* **127**, 3.  
 DAVIES, R. D., and GARDNER, F. F. (1966).—*Aust. J. Phys.* **19**, 823.  
 DAVIS, M. M., GELATO-VOLDERS, L., and WESTERHOUT, G. (1965).—*Bull. astr. Insts Neth.* **18**, 42.  
 EDGE, D. O., SHAKESHAF, J. R., McADAM, W. B., BALDWIN, J. E., and ARCHER, S. (1958).—*Mem. R. astr. Soc.* **68**, 37.  
 EKERS, R. D. (1969).—*Aust. J. Phys. astrophys. Suppl.* No. 6.  
 GOWER, J. F. R., SCOTT, P. F., and WILLS, D. (1967).—*Mem. R. astr. Soc.* **71**, 49.  
 HILL, E. R. (1967).—*Aust. J. Phys.* **20**, 297.  
 HILL, E. R. (1968).—*Aust. J. Phys.* **21**, 735.  
 HOLLINGER, J. P., and HOBBS, R. W. (1966).—*Science, N.Y.* **153**, 1633.  
 KESTEVEN, M. J. L. (1968a).—*Aust. J. Phys.* **21**, 369.  
 KESTEVEN, M. J. L. (1968b).—*Aust. J. Phys.* **21**, 739.  
 KOMESAROFF, M. M. (1966).—*Aust. J. Phys.* **19**, 75.  
 KUZMIN, A. D. (1962).—*Soviet Astr. AJ* **5**, 692.  
 LESLIE, P. R. R. (1960).—*Observatory* **80**, 23.  
 MATHEWSON, D. S., HEALEY, J. R., and ROME, J. M. (1962).—*Aust. J. Phys.* **15**, 354.  
 MILLS, B. Y., SLEE, O. B., and HILL, E. R. (1958).—*Aust. J. Phys.* **11**, 360.  
 MILLS, B. Y., SLEE, O. B., and HILL, E. R. (1960).—*Aust. J. Phys.* **13**, 676.  
 MILLS, B. Y., SLEE, O. B., and HILL, E. R. (1961).—*Aust. J. Phys.* **14**, 497.  
 MILNE, D. K. (1968a).—*Proc. astr. Soc. Aust.* **1**, 93.  
 MILNE, D. K. (1968b).—*Aust. J. Phys.* **21**, 201.  
 MILNE, D. K., and HILL, E. R. (1969).—*Aust. J. Phys.* **22**, 211.  
 MORAN, J. M. (1965).—*Mon. Not. R. astr. Soc.* **129**, 447.  
 MORIMOTO, M., and LOCKHART, I. A. (1968).—*Proc. astr. Soc. Aust.* **1**, 99.  
 PAULINY-TOH, I. I. K., WADE, C. M., and HEESCHEN, D. S. (1966).—*Astrophys. J. Suppl. Ser.* **13**, 65.  
 REIFENSTEIN III, E. C. (1968).—Ph.D. Thesis, Massachusetts Institute of Technology.  
 SCHEUER, P. A. G. (1963).—*Observatory* **83**, 56.  
 WESTERHOUT, G. (1958).—*Bull. astr. Insts Neth.* **14**, 215.  
 WILSON, R. W. (1963).—*Astr. J.* **68**, 181.